The Journal of Experimental Biology 204, 3765–3777 (2001)
Printed in Great Britain © The Company of Biologists Limited 2001
JEB3654

The energetics of rat papillary muscles undergoing realistic strain patterns

L. J. Mellors* and C. J. Barclay
Department of Physiology, PO Box 13F, Monash University, Victoria 3800, Australia
*e-mail: Linda.Mellors@med.monash.edu.au

Accepted 9 August 2001

Summary

Studies of cardiac muscle energetics have traditionally used contraction protocols with strain patterns that bear little resemblance to those observed *in vivo*. This study aimed to develop a realistic strain protocol, based on published *in situ* measurements of contracting papillary muscles, for use with isolated preparations. The protocol included the three phases observed in intact papillary muscles: an initial isometric phase followed by isovelocity shortening and re-lengthening phases. Realistic papillary muscle dynamics were simulated *in vitro* (27 °C) using preparations isolated from the left ventricle of adult male rats. The standard contraction protocol consisted of 40 twitches at a contraction rate of 2 Hz. Force, changes in muscle length and changes in muscle temperature were measured simultaneously. To quantify the energetic costs of contraction, work output and enthalpy output were determined, from which the maximum net mechanical efficiency could be calculated. The most notable result from these experiments was the constancy of enthalpy output per twitch, or energy cost, despite the various alterations made to the protocol. Changes in mechanical efficiency, therefore, generally reflected changes in work output per twitch. The variable that affected work output per twitch to the greatest extent was the amplitude of shortening, while changes in the duration of the initial isometric phase had little effect. Decreasing the duration of the shortening phase increased work output per twitch without altering enthalpy output per twitch. Increasing the contraction frequency from 2 to 3 Hz resulted in slight decreases in the work output per twitch and in efficiency. Using this realistic strain protocol, the maximum net mechanical efficiency of rat papillary muscles was approximately 15 %. The protocol was modified to incorporate an isometric relaxation period, thus allowing the model to simulate the main mechanical features of ventricular function.

Key words: mechanical efficiency, heat production, enthalpy output, work loop, cardiac muscle, rat, muscle.

Introduction

The role of the left ventricular papillary muscles is to provide structural support to the mitral valve during cardiac contraction. The muscles are particularly important for valve closure during systole, ensuring that the valve does not protrude into the atrium; e.g. Cronin et al. (Cronin et al., 1969) and Marzilli et al. (Marzilli et al., 1980). Several studies have mapped the strain pattern of papillary muscles *in situ* (Armour and Randall, 1970; Cronin et al., 1969; Gorman et al., 1996; Hirakawa et al., 1977; Marzilli et al., 1985; Rayhill et al., 1994; Semafuko and Bowie, 1975). The typical strain time course measured in these studies can be separated into three phases: an initial isometric phase that occurs during isovolumic contraction at the start of systole, a shortening phase occurring during ejection (ventricular emptying) and a re-lengthening phase that coincides with the filling of the relaxed ventricle.

In vitro studies of cardiac energetics have traditionally used the papillary muscle as a model of ventricular muscle. The protocols used in these types of studies have usually involved either isometric or afterloaded isotonic contractions (Gibbs and Chapman, 1979; Gibbs et al., 1967; Kiriazis and Gibbs, 1995; Kiriazis and Gibbs, 2000). Neither of these protocols results in a net output of mechanical work, and typically the contraction frequency is very low compared with physiological frequencies. These and other interpretative difficulties have been discussed extensively by Mellors et al. (Mellors et al., 2001).

Semafuko and Bowie (Semafuko and Bowie, 1975) highlighted the lack of correspondence between the strain patterns used in traditional *in vitro* studies and those measured from papillary muscles *in situ*. However, there have still been no studies of papillary muscle mechanics or energetics using realistic strain protocols and contraction frequencies. With current technology, it is possible to simulate *in vivo* papillary muscle strain patterns *in vitro*.

Two recent studies from this laboratory (Baxi et al., 2000; Mellors et al., 2001) employed a sinusoidal length change protocol as an approximation of *in vivo* papillary muscle contraction. This protocol did produce more realistic patterns of force and length changes, was performed at realistic contraction frequencies and resulted in net work output.

However, the sinusoidal strain pattern, although more realistic than isometric or isotonic contractions, is still a relatively poor match to *in situ* strains.

The aims of the current study were (i) to determine, from published reports, a typical strain pattern of *in situ* papillary muscles, (ii) to incorporate this pattern into a contraction protocol for isolated papillary muscle preparations and (iii) to characterise the energetics of rat papillary muscles performing the realistic length change protocol. Because there is some variation in the fine details of the *in situ* strain pattern, the pattern of length changes used in this study was varied to encompass the most likely patterns.

A comprehensive search of the literature describing *in situ* papillary muscle strain dynamics revealed that the muscles undergo cyclic length changes during contraction [e.g. Cronin et al. (Cronin et al., 1969), Marzilli et al. (Marzilli et al., 1985), Rayhill et al. (Rayhill et al., 1994) and Semafuko and Bowie (Semafuko and Bowie, 1975)] and shorten by approximately 10 % of their resting length at a fairly constant velocity (Gorman et al., 1996; Hirakawa et al., 1977; Semafuko and Bowie, 1975). Some reports identified a brief period of isometric contraction at the start of ventricular systole (Armour and Randall, 1970; Hirakawa et al., 1977; Karas and Elkins, 1970; Rayhill et al., 1994), but the duration of this phase was variable. Other studies have reported that muscle length increased by a small amount at the beginning of ventricular systole rather than remaining isometric (Cronin et al., 1969; Marzilli et al., 1985; Semafuko and Bowie, 1975). Both these possibilities were encompassed by the protocols used in the present study. Following shortening, re-extension of the muscles to the length recorded at the start of each cycle also occurred at an approximately constant velocity.

Materials and methods

The procedures involved in obtaining left ventricular papillary muscle preparations from adult male rats (Sprague-Dawley strain; 12–16 weeks old) have been described previously (Mellors et al., 2001). The methods of obtaining force, muscle length change and muscle heat output measurements have also been described in detail (Barclay, 1994; Barclay et al., 1995; Baxi et al., 2000; Mellors et al., 2001). Briefly, papillary muscles were mounted in a bath between a force transducer and a servo-controlled motor. The muscle lay along a thermopile that was used to measure changes in muscle temperature, from which heat production could be calculated. The thermopile used in this study contained 24 antimony/bismuth thermocouples and had an active recording length of 6 mm and an output of 1.09 mV °C^{-1}. Temperature recordings were converted to heat output by first correcting the recording for heat lost through the thermocouple wires to the frame and then multiplying the corrected temperature by the muscle's heat capacity. The rate of heat loss and muscle heat capacity were calculated from the time course of cooling of the preparation following a period of heating using the Peltier effect (Kretzschmar and Wilkie, 1972; Woledge et al., 1985).

The total enthalpy output from a contracting muscle is the sum of the heat and work outputs. Net work output during a contraction was calculated by integrating force with respect to the change in muscle length (i.e. net work output is equal to the area enclosed by a plot of force as a function of change in muscle length). This calculation determines the difference between the total work performed by the muscle during shortening and that performed on the muscle to re-lengthen it prior to starting the next length change cycle.

Experimental protocols

Once mounted, each preparation was set to the length at which active force production was maximal (L_{max}). Muscles then performed isometric contractions at L_{max} for 1.5 h at a rate of 0.2 Hz to allow mechanical performance to stabilise. The muscle preparation was kept at 27 °C throughout the experiment. It has been shown previously, by modelling the diffusion of O_2 into cylindrical muscles, that at this temperature diffusive O_2 supply would be adequate to meet the metabolic needs of papillary muscles contracting at the frequencies used in this study (Baxi et al., 2000). At higher temperatures, it is possible that the O_2 supply may not be adequate, leading to the formation of an anoxic region in the centre of the preparations.

Recordings of muscle enthalpy output were made with the muscle out of solution. Stimulation of the muscle ceased prior to drainage to allow any heat generated by the muscle during stimulation to dissipate into the solution. The muscle remained unstimulated for approximately 8 min prior to experimental recordings to allow the thermopile output to stabilise. The standard experimental protocol used in this study consisted of 40 twitches at a contraction rate of 2 Hz. The muscle was re-immersed in solution and stimulated at 0.2 Hz for 20 min between sets of measurements. At all times during experiments, the chamber containing the muscle was supplied with 95 % O_2/5 % CO_2.

Three experiments were performed. Experiment 1 investigated the effects of varying the strain dynamics, experiment 2 investigated the effects of varying the shortening duration at constant frequency and experiment 3 investigated the effects of varying the frequency of contraction while maintaining a constant duration of shortening.

Experiment 1: varying strain dynamics

In the first experiment, two aspects of the strain dynamics were investigated. First, the effects of varying the duration of the isometric phase at the start of contraction were studied. The duration was set to 10, 15 or 20 % of the cycle duration (one cycle is the interval between successive stimuli) (Fig. 1A). The consequences of incorporating an increase in muscle length (2 or 4 % L_{max}) before the onset of shortening (15 % cycle duration) were also studied (Fig. 1B). Second, the amplitude of shortening was varied such that it equalled 5, 10 or 15 % L_{max} (Fig. 1C). Each shortening amplitude was preceded by an isometric contraction accounting for 10, 15 or 20 % of the cycle duration.

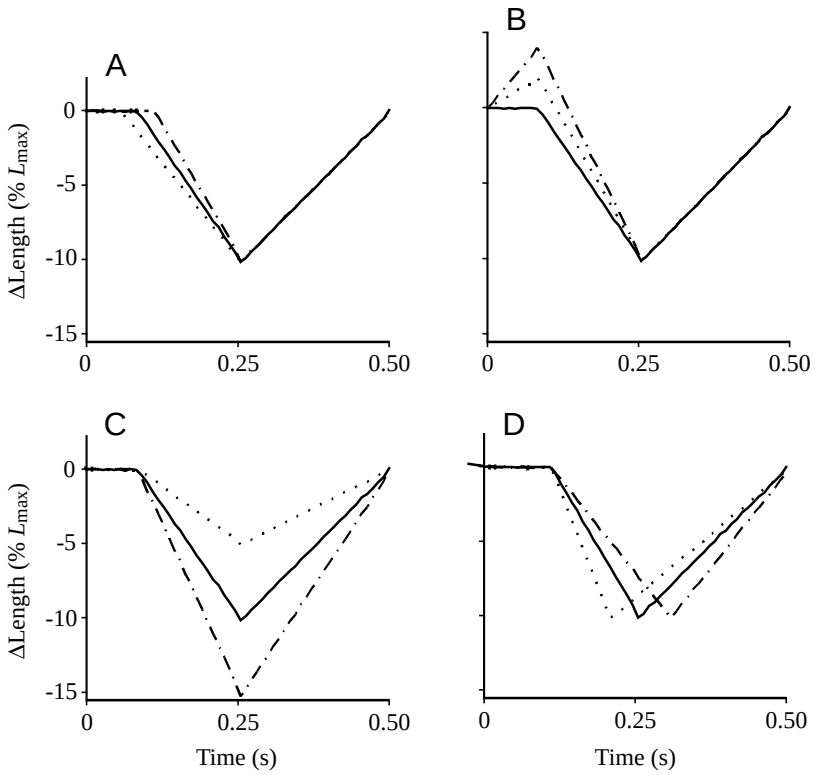

Fig. 1. Examples of muscle length changes (ΔLength) during realistic contraction protocols at 2 Hz. A, B and C show the length change protocols for experiment 1 and D for experiment 2. In A, the duration of initial isometric contraction was 10, 15 or 20 % of the total inter-stimulus interval (0.5 s) (shown for 10 % L_{max} shortening only), where L_{max} is the length at which active force production is maximal. In B, the isometric phase was substituted by a 2 or 4 % L_{max} length increase, accounting for 15 % of the cycle duration. At each isometric duration, the muscle was shortened by 5, 10 or 15 % L_{max} (shown for an isometric duration of 15 % of the cycle only) (C). The duration of the lengthening phase was kept at 50 % of the cycle duration in A, B and C. In D, isometric phase duration was 20 % of the cycle duration, while shortening was for 20, 30 or 40 % of the inter-stimulus interval. The duration of the lengthening phase was adjusted accordingly. Shortening amplitude was 10 % L_{max} in B and D. The stimulus pulse was applied at time zero.

Experiment 2: varying the shortening duration at constant frequency

A series of experiments was performed to determine whether altering the shortening duration at constant frequency affected the energetic characteristics of the muscle. The pattern of length changes was altered such that the shortening phase accounted for 20, 30 or 40 % of the inter-stimulus interval (Fig. 1D). Isometric contraction duration was constant at 20 % of cycle duration, and the duration of the lengthening phase was altered as required to maintain the cycle duration at 500 ms.

Experiment 3: varying contraction frequency

A contraction frequency of 2 Hz was selected as the basic frequency for this study. In a recent report on the energetics of rat papillary muscle, this frequency was found to be within the range for maximum work output and maximum net mechanical efficiency (Baxi et al., 2000). In addition, a number of experiments were performed at a contraction rate of 3 Hz. This 50 % increase in heart rate is comparable with the range of heart rate increases that occurs between rest and vigorous exercise in rats; e.g. Drexler et al. (Drexler et al., 1985) and Mullin et al. (Mullin et al., 1984). The total durations of the isometric and shortening phases were kept constant, while the duration of the lengthening phase was reduced for the contractions at 3 Hz (Miyazaki et al., 1990). Thus, the absolute duration of the combined isometric and shortening phase was the same in the 2 and 3 Hz contraction protocols.

Measurement of the stiffness of the series elastic component

In experiment 1, the velocity of shortening of the muscle was varied. To assess the probable effects of these alterations in whole-muscle shortening velocity on the velocity of the contractile component alone, the contractile component velocity was calculated using the following equation (Curtin and Woledge, 1993):

$$V_{CC} = V_L - \left(\frac{1}{S} \times \frac{dP}{dT}\right), \quad (1)$$

where V_{CC} is the shortening velocity of the contractile component, V_L is the shortening velocity of the whole muscle, S is the stiffness of the series elastic component (SEC) (which varied with force) and dP/dt is the rate of change in force.

The stiffness of the SEC of papillary muscle preparations was measured using the method described by Sonnenblick (Sonnenblick, 1964). Each muscle performed isotonic twitches (10 twitches at 0.2 Hz) against a series of afterloads between $0.2P_0$ and $0.8P_0$, where P_0 is the maximum isometric twitch force (excluding passive force). Afterloaded isotonic twitches involve the muscle contracting isometrically until the force reaches the desired afterload, then shortening and re-lengthening while force output remains constant, and then relaxing isometrically (Fig. 2). Two runs were performed on each muscle with loads presented alternately in ascending and descending order. The required afterload was achieved using an adaptive force control algorithm (Mellors et al., 2001; Peterson et al., 1989). For each muscle at each load, the stiffness of the SEC (S) was calculated using the expression (Sonnenblick, 1964):

$$S = dP/dL = (dP/dt)/(dL/dt), \quad (2)$$

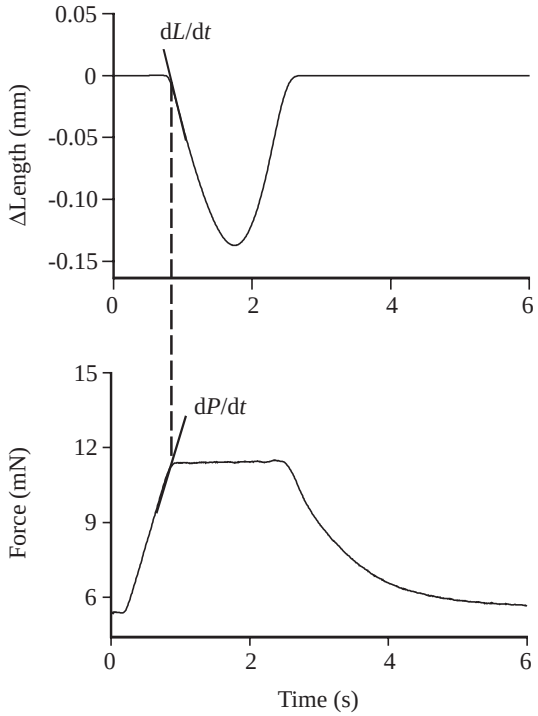

Fig. 2. Recordings of force output (lower trace) and muscle length change (ΔLength) (upper trace) during an isotonic contraction illustrating the method used to determine the stiffness of the series elastic component. The example shown is from a muscle shortening against a load of $0.6P_0$, where P_0 is the maximum isometric twitch force. The dashed vertical line indicates the time at which shortening started. The solid straight lines were fitted to the muscle length change trace (upper trace) at the start of shortening and to the force trace (lower trace) immediately before shortening started. The slopes of these lines give the initial velocity of shortening (dL/dt) and rate of force development just prior to shortening (dP/dt), respectively. The ratio of dP/dt to dL/dt gives the stiffness of the elastic component in series with the contractile element at that load. The sampling rate for these experiments was 1000 Hz.

where dP/dt is the rate of force development immediately prior to the start of shortening and dL/dt the initial velocity of shortening (Fig. 2).

Calculations

Data normalisation

The blotted wet mass of each preparation was determined at the conclusion of each experiment (Mellors et al., 2001). Muscle force was normalised by cross-sectional area (CSA), which was calculated as mass/(length×density), assuming a density of $1.06\,g\,cm^{-3}$ (Hill, 1931).

Net mechanical efficiency

Net mechanical efficiency (ε_{Net}) was defined as the percentage of the total, suprabasal enthalpy output (H_{Total}) that appeared as external, mechanical work:

$$\varepsilon_{Net} = (W_{Total}/H_{Total}) \times 100\,, \quad (3)$$

where W_{Total} was the sum of the net work output produced in each contraction in the series and H_{Total} was the total suprabasal enthalpy output (i.e. heat + work) and included metabolism due to both initial (i.e. ATP-utilizing) and recovery (i.e. ATP-synthesising) biochemical reactions.

Table 1. *Characteristics of papillary muscle preparations*

Wet mass (mg)	2.87±0.27
L_{max} (mm)	4.96±0.19
Cross-sectional area at L_{max} (mm^2)	0.54±0.04
Passive force at L_{max} (mN)	4.6±0.5
Isometric active force at L_{max} (mN)	14.0±1.2
Active stress at L_{max} ($mN\,mm^{-2}$)	26.9±1.7
Passive force/active force at L_{max}	0.35±0.04
Isometric enthalpy output at L_{max} ($mJ\,g^{-1}$)	7.5±1.7

All values are mean ± 1 S.E.M. (N=12, except for isometric enthalpy output where N=4).

Statistical analyses

All data are presented as the mean ±1 S.E.M. Data were analysed using analysis of variance (ANOVA) with repeated measures. *Post-hoc* testing was performed using the least significant difference test. All decisions concerning statistical significance were made at the 95 % confidence level.

Results

The aims of this study were to develop a contraction protocol for use with isolated papillary muscles that mimicked papillary muscle length changes measured *in situ* and to characterise the energetics of rat papillary muscles using this protocol. The general characteristics of the papillary muscle preparations are presented in Table 1.

Typical recordings from a realistic contraction protocol are illustrated in Fig. 3. It can be seen that peak force output varied during the 40 twitches, with the first twitch exhibiting a high peak force output, as typically observed in rat cardiac muscle following a period of quiescence (Ravens, 1992). The muscle temperature increased progressively throughout the contraction protocol and, once stimulation ceased, decreased back to its initial value within approximately 1 min. The decrease in temperature reflects the net effect of heat flowing from the muscle through the metals of the thermocouples to the thermopile frame and the ongoing metabolic heat production that follows a period of activity. Muscle temperature returns to its initial value only when the rate of metabolic heat production is equal to the rate before commencement of the contraction protocol. The lowest panel shows the calculated cumulative work, heat and enthalpy outputs.

Experiment 1: varying strain dynamics

In experiment 1, the effects of varying the amplitude of muscle shortening and the duration of the initial isometric phase were determined. Examples of work loops for these protocols are shown in Fig. 4.

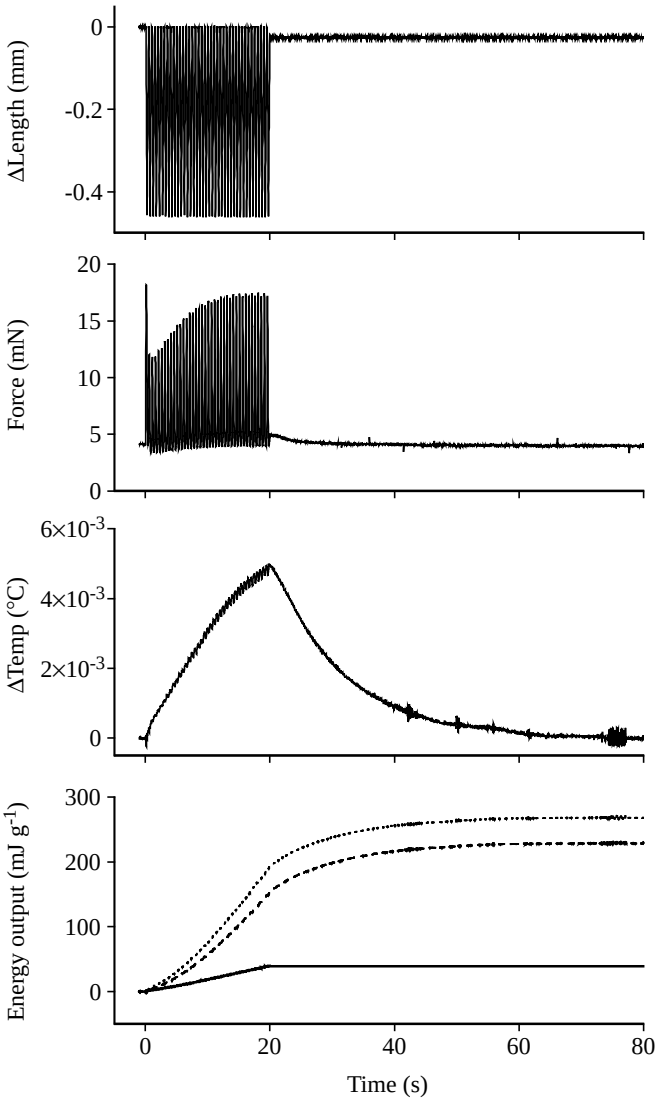

Fig. 3. Examples of recordings made during a realistic contraction protocol. The recordings shown are (from top to bottom): change in muscle length (ΔLength), force output, change in muscle temperature (ΔTemp) and cumulative work (solid line), heat (dashed line) and enthalpy (dotted line) outputs. The enthalpy output is the sum of the work and heat outputs. The muscle returned to its pre-stimulation temperature within 1 min of completion of the contractions, indicating that all recovery metabolism was complete. Muscle mass, 3.58 mg; length, 4.5 mm, cross-sectional area, 0.75 mm^2.

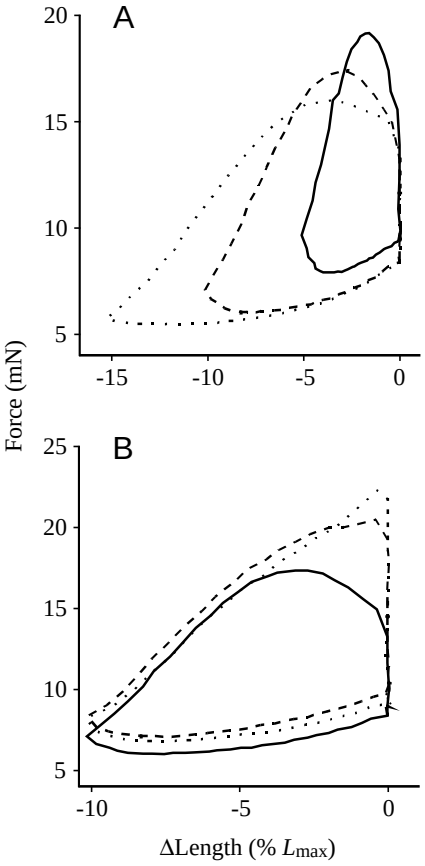

Fig. 4. Examples of work loops. (A) The duration of the initial isometric contraction was 10 % of the cycle duration, and the amplitude of shortening was 5 % L_{max} (solid line), 10 % L_{max} (dashed line) or 15 % L_{max} (dotted line), where L_{max} is the length at which active force production is maximal. The duration of the lengthening phase was constant. Therefore, the velocity of shortening increased as the amplitude of shortening increased. (B) The amplitude of shortening was 10 % L_{max} and the duration of the lengthening phase was 50 % of the cycle duration. The duration of the initial isometric phase was 10 % (solid line), 15 % (dashed line) or 20 % (dotted line) of the cycle duration. Time progressed around the loops in an anticlockwise direction, indicating that net work was performed. ΔLength, change in muscle length.

Increasing the amplitude of shortening increased the work output per twitch, as shown by the increase in size of the work loops in Fig. 4A. The enthalpy output per twitch, however, remained constant (Fig. 5B). The consequence of an increase in work output accompanied by little change in enthalpy output was that net mechanical efficiency increased significantly with increased shortening amplitude.

The only energetic consequence of increasing the duration of the isometric phase was that an increase in duration from 10 to 15 % increased work output and enthalpy output when the shortening amplitude was 10 or 15 % L_{max} (Fig. 5). Extending the isometric phase to 20 % of the cycle duration had no further effect, and when shortening was 5 % L_{max}, neither work output nor enthalpy production was affected by the duration of the initial isometric contraction. There were no significant effects of isometric duration on ε_{Net}. Note that the mean enthalpy output per twitch in Fig. 5B was similar to the mean enthalpy output measured in an isometric twitch (Table 1).

Applying an initial stretch instead of holding the muscle isometric at the beginning of the contraction did not affect enthalpy output (Fig. 6). The work output per twitch, however, did increase with a greater magnitude of length increase (isometric, 1.04±0.12 mJ g^{-1}; 2 % L_{max} increase, 1.15±0.12 mJ g^{-1}; 4 % L_{max} increase, 1.29±0.14 mJ g^{-1}). There was no significant difference in ε_{Net} between the contractions with an initial isometric phase (12.5±0.6 %) and those with a

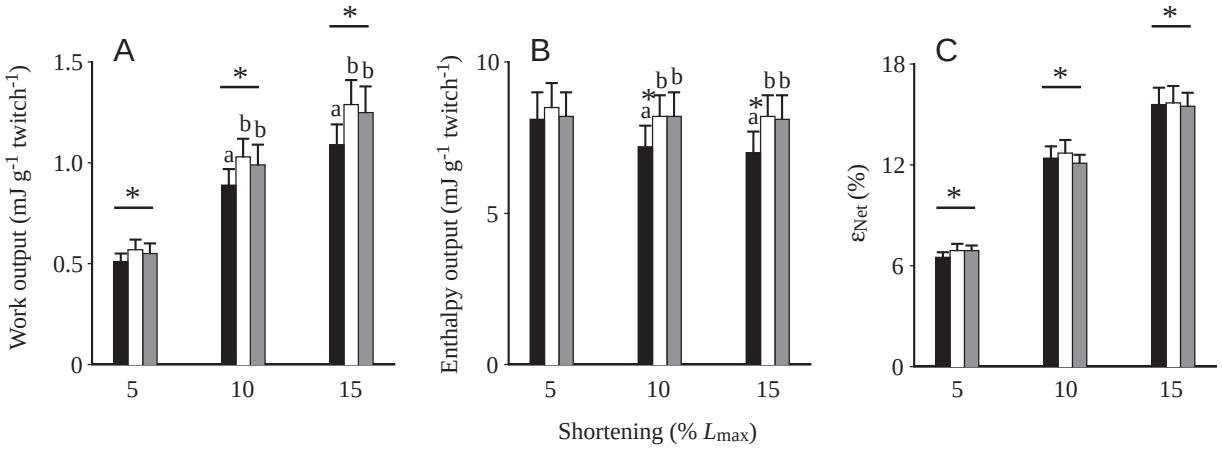

Fig. 5. Effects of varying the shortening amplitude (%L_{max}, where L_{max} is the length at which active force production is maximal) and the duration of isometric contraction (percentage cycle duration) on mean work output per cycle (A), enthalpy output per cycle (B) and net mechanical efficiency, ε_{Net} (C). The duration of isometric contraction was 10 % (black columns), 15 % (white columns) or 20 % (grey columns) of the cycle duration. Letters indicate statistically significant differences between variables attributable to the duration of isometric contraction. Asterisks indicate statistical significance, at a particular isometric duration, attributable to shortening amplitude. Values are means + S.E.M., N=7.

2 %L_{max} increase in length (13.0±1.1 %). However, ε_{Net} was significantly greater (14.6±1.2 %) when a 4 %L_{max} increase in length was incorporated into the protocol in place of either a 0 or 2 %L_{max} length increase.

Experiment 2: varying shortening duration at constant frequency

In this experiment, the cycle duration was constant (500 ms=2 Hz) as was the initial isometric phase (100 ms, 20 % of cycle duration). The duration of the shortening phase was 100, 150 or 200 ms (20, 30 or 40 % of cycle duration respectively), and the duration of the lengthening phase was adjusted accordingly. Thus, the velocity of shortening varied between 0.5 $L_{max}\,s^{-1}$ and 1.0 $L_{max}\,s^{-1}$. The maximum shortening velocity of rat papillary muscle is 6.5 $L_{max}\,s^{-1}$ at 37 °C (Henderson et al., 1970), which would correspond to approximately 3.25 $L_{max}\,s^{-1}$ at 27 °C, assuming a halving of velocity for a decrease in temperature of 10 °C. Despite the variation in shortening velocity, the enthalpy output, or energetic cost of contraction, was independent of the shortening duration (Fig. 7). However, less work was performed per twitch when the lowest shortening velocity was used than at either of the other velocities. This was due to the force relaxing to resting levels before shortening was complete, reducing the net work performed. Consequently, ε_{Net} was significantly lower when shortening lasted for 200 ms (11.0±0.7 %) than for 100 ms (13.5±0.7 %) or 150 ms (12.1±0.5 %).

Experiment 3: varying contraction frequency

Work output per twitch was significantly lower when the contraction frequency was increased from 2 Hz (1.09±0.12 mJ g^{-1}) to 3 Hz (0.89±0.08 mJ g^{-1}) (Fig. 8). The mean enthalpy output per twitch was slightly, but not significantly, reduced from 8.3±0.8 mJ g^{-1} at 2 Hz to 7.5±0.5 mJ g^{-1} at 3 Hz. The overall result was that ε_{Net} was slightly, but significantly, lower at 3 Hz (11.9±1.1 %) compared with 2 Hz (13.2±0.8 %).

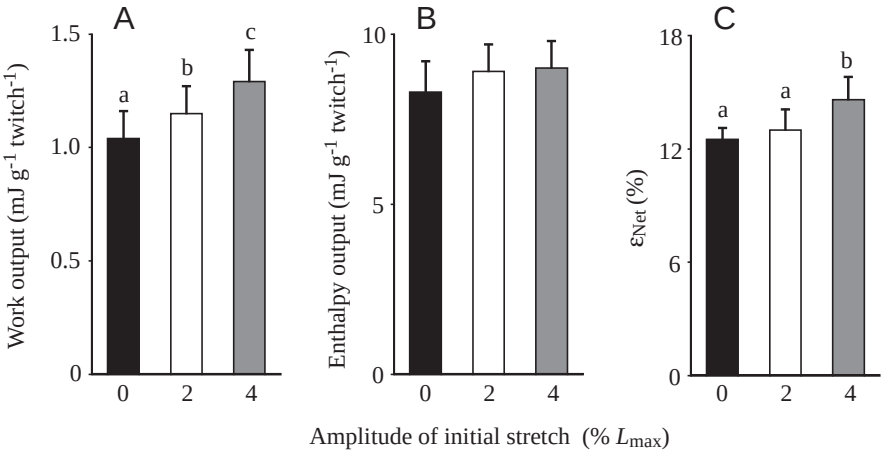

Fig. 6. Effects of incorporating an initial stretch in place of the initial isometric period on mean work output per cycle (A), enthalpy output per cycle (B) and net mechanical efficiency, ε_{Net} (C) (N=6). The duration of the initial stretch or isometric period was 75 ms or 15 % of the cycle duration, and shortening was 10 %L_{max}, where L_{max} is the length at which active force production is maximal. Letters indicate statistically significant differences. Values are means + S.E.M.

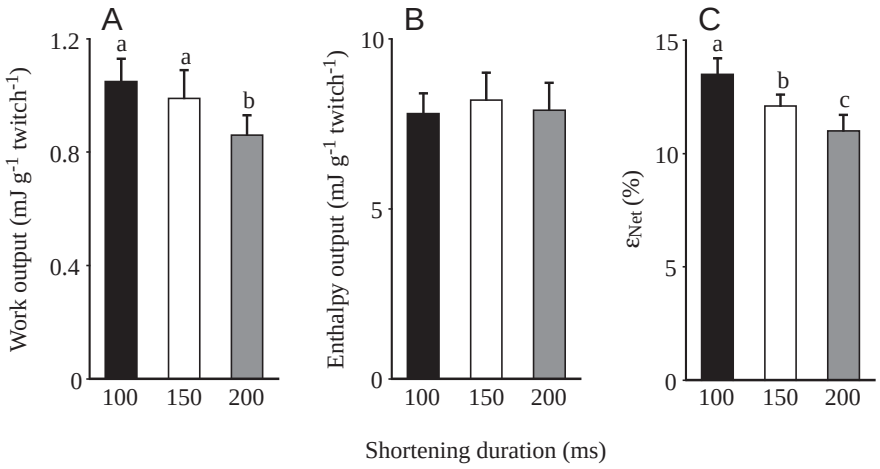

Fig. 7. Effects of varying the shortening duration of contractions on mean work output per cycle (A), enthalpy output per cycle (B) and net mechanical efficiency, ε_{Net} (C) (N=7). Isometric phase duration was 100 ms. Letters indicate statistically significant differences. Values are means + S.E.M.

Are steady-state and non-steady-state energetics comparable?

In vivo, the heart works at an energetic steady state; that is, ATP is synthesised at a rate sufficient to match ATP use. In the 40-twitch protocol used in the current study, the muscle progressed from rest to steady activity, but reached an energetic steady state only near the end of the protocol. An energetic steady state can be implied when the pattern of temperature changes repeats in successive cycles (Paul, 1983). To ensure that steady-state energetics are similar to those during the rest-to-work transition, recordings were made during a protocol consisting of 60 twitches at 2 Hz (Fig. 9).

The average work performed per twitch and enthalpy output per twitch were slightly, but significantly, lower in the 60-twitch protocol than in the 40-twitch protocol. There was, however, no effect on ε_{Net} (12.5±0.8 %; 60 twitches compared with 12.7±0.8 %; 40 twitches) (N=7). Note that, to compare the steady-state and non-steady-state energetics, it was necessary to record the total enthalpy output (i.e. including recovery metabolism) from both 40- and 60-twitch protocols.

Using the protocol as a model of ventricular muscle

The shapes of the force/length loops in Fig. 4 differ from ventricular pressure/volume loops in that the latter generally exhibit a clear isovolumic relaxation phase [for a comprehensive review, see Sagawa et al. (Sagawa et al., 1988)]. It is unclear, from *in situ* strain and length change recordings, whether the papillary muscles remain isometric during the isovolumic relaxation phase, with reports indicating varying degrees of shortening (Hirakawa et al., 1977; Marzilli et al., 1985; Semafuko and Bowie, 1975), lengthening (Rayhill et al., 1994) or no significant length change (Hirakawa et al., 1977; Rayhill et al., 1994). Regardless of the disagreement in the literature, if papillary muscles are to be used as a linear model of ventricular muscle, the addition of an isometric relaxation phase would enhance the realism of the model. To determine whether this feature could easily be incorporated into the protocols used in this study, an experiment was carried out in which the muscle length was held constant during part of the relaxation phase. The isometric relaxation phase was incorporated into the length change pattern by selecting a time for shortening to end and by holding the length constant until relaxation was complete (Fig. 10). The results from these experiments are shown in Table 2. As the absolute shortening amplitude was increased, work output per twitch also increased. This result is in agreement with the findings of experiment 1. Once again, the enthalpy output per twitch varied over only a small range and, thus, ε_{Net} reflected the variation in work output.

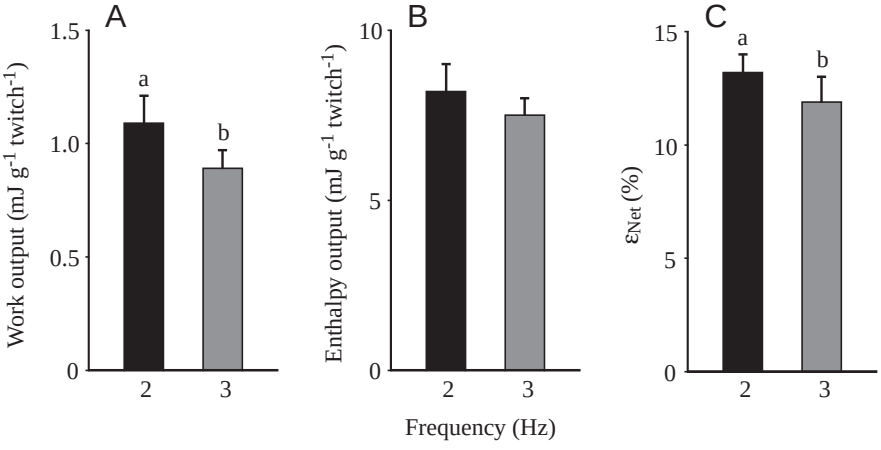

Fig. 8. Effects of varying contraction frequency on mean work output per cycle (A), enthalpy output per cycle (B) and net mechanical efficiency, ε_{Net} (C) (N=6). The duration of the initial stretch or isometric period was 75 ms or 15 % of the cycle duration, and shortening was 10 % L_{max}, where L_{max} is the length at which active force production is maximal. Letters indicate statistically significant differences. Values are means ± S.E.M.

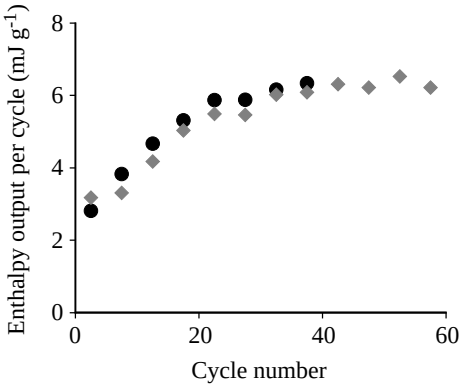

Fig. 9. Example of the time course of enthalpy output from a muscle performing 40 (circles) and 60 (diamonds) realistic contractions at 2 Hz. Isometric contraction was 15 % of the cycle duration, while shortening and lengthening phases accounted for 35 % and 50 % of the cycle duration respectively. Data points represent the mean enthalpy output per cycle averaged over five successive cycles. The horizontal position of each data point corresponds to the middle of the cycles over which the mean values were calculated.

Stiffness of the series elastic component and its effects on contractile component shortening velocity

Five papillary muscle preparations were used to measure the stiffness of the SEC. SEC stiffness increased linearly with load (Fig. 11). The slope of the stiffness/load relationship was determined for each preparation, and the mean value was 3.42±0.17 mm^{-1} (mean muscle length was 6.1±0.3 mm). The linear dependence of stiffness on load implies an exponential dependence of extension of the SEC on load, as described previously for papillary muscles (Sonnenblick, 1964). The purpose of making these measurements was to enable the velocity of the contractile component during shortening to be calculated and to be compared with the overall velocity of shortening (equation 1).

A quantitative assessment was made of the time course of shortening of the contractile component in realistic contractions. This analysis was performed for applied shortenings of 5, 10 and 15 % L_{max} and tested whether the effect of the SEC caused the velocity profiles of the contractile component to be similar for all three shortening magnitudes despite the differences in the velocity profile of the length changes applied to the ends of the muscle. If this were so, then the constancy of the enthalpy output per twitch (e.g. Fig. 5B) might simply reflect the similar pattern of contractile length changes.

An example of the results of this analysis is shown in Fig. 12A. The time course of changes in length of the whole muscle (controlled by the experimenter) is compared with the time courses of length changes in the contractile component and the SEC. The first notable feature is that the contractile component began to shorten and stretch the SEC as soon as the contraction started, as reported previously (Brady, 1971; Donald et al., 1980). In fact, in this example, in which the initial 'isometric' phase lasted 100 ms, the contractile component had

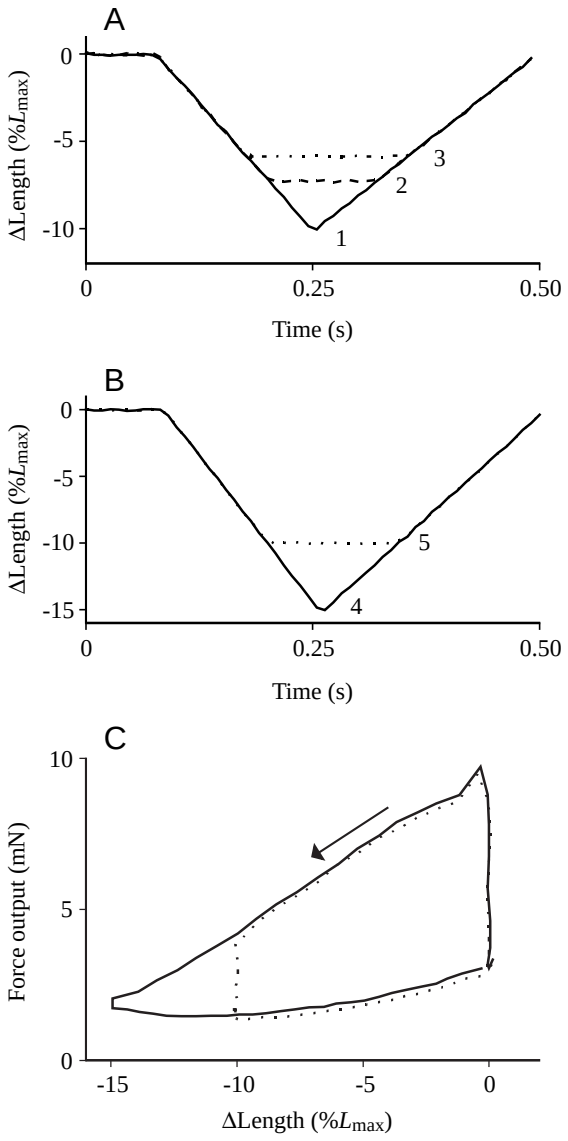

Fig. 10. Examples of muscle length changes (ΔLength) (A,B) and work loops (C) during realistic contractions with (dotted lines) or without (solid lines) an isometric relaxation period. The length changes shown in A are from a muscle shortening by 10 % L_{max}, where L_{max} is the length at which active force production is maximal, or incorporating an isometric relaxation period such that the absolute amplitude of shortening was less than 10 % L_{max}. The length changes pictured in B are similar to those in A, except that the maximum amplitude of shortening was 15 % L_{max}. The work loops in C correspond to the length changes in B. The numbers beside the traces correspond to the contraction types listed in Table 2.

shortened by approximately 5 % L_{max} before the applied shortening even started. During the applied constant-velocity shortening, the velocity of the contractile component was not constant but decreased steadily and reached almost zero by the time the applied shortening ended. During the subsequent re-lengthening, changes in the length of the contractile component and the whole preparation were quite similar because the rate of change in force was very low during this phase.

Table 2. *Effects of incorporating an isometric relaxation period on energetic variables*

	Contraction type				
	1	2	3	4	5
Work (mJ g^{-1} twitch^{-1})	1.14±0.11	1.08±0.13	0.92±0.09	1.34±0.14	1.24±0.10
Enthalpy (mJ g^{-1} twitch^{-1})	7.6±1.2	8.0±1.6	8.4±1.9	7.4±1.2	7.9±1.9
ε_{Net} (%)	15.4±1.3	14.1±1.4	11.9±1.2	18.8±1.3	17.0±2.0

All values are presented as mean ± S.E.M. (N=4). Contraction type corresponds to length change patterns illustrated in Fig. 10.
ε_{Net}, net mechanical efficiency.
Contraction types: 1, 10 % L_{max} shortening, no isometric relaxation; 2, isometric relaxation after 7.3 % L_{max} shortening; 3, isometric relaxation after 5.8 % L_{max} shortening; 4, 15 % L_{max} shortening, no isometric relaxation; 5, isometric relaxation after 10 % L_{max} shortening.

In Fig. 12B,C, the time courses of the applied length changes for the three amplitudes of shortening are compared with the calculated contractile component length changes. Irrespective of the strain pattern, the first 5 % L_{max} shortening of the contractile component had occurred before any change in preparation length. Thus, during this initial phase, the contractile component shortened at the same velocity and through the same amplitude in all three examples. During the time that the muscle length was being decreased, contractile component length continued to decrease at progressively lower velocities. The total amplitude of contractile component shortening was affected by the amplitude of the applied length change, but not in a simple way. For instance, when the whole muscle was shortened by 5 % L_{max}, the calculated amplitude of contractile shortening was actually approximately 7 % L_{max}. When the applied length change had an amplitude of 15 % L_{max}, the calculated contractile component shortening amounted to approximately 13 % L_{max}. The difference in these length changes is accounted for by changes in the length of the SEC.

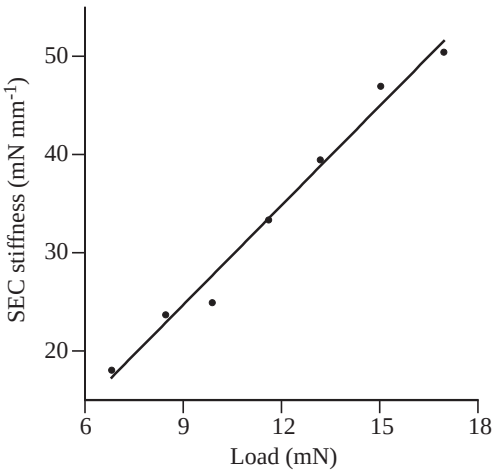

Fig. 11. Example of the relationship between afterload and the stiffness of the series elastic component (SEC). The range of loads for this preparation (length 6.1 mm) corresponded to 0.2–0.8P_0, where P_0 is the maximum isometric twitch force. The line was fitted through the data using the method of least squares (r^2=0.984). The method used to calculate stiffness is described in Materials and methods and illustrated in Fig. 2.

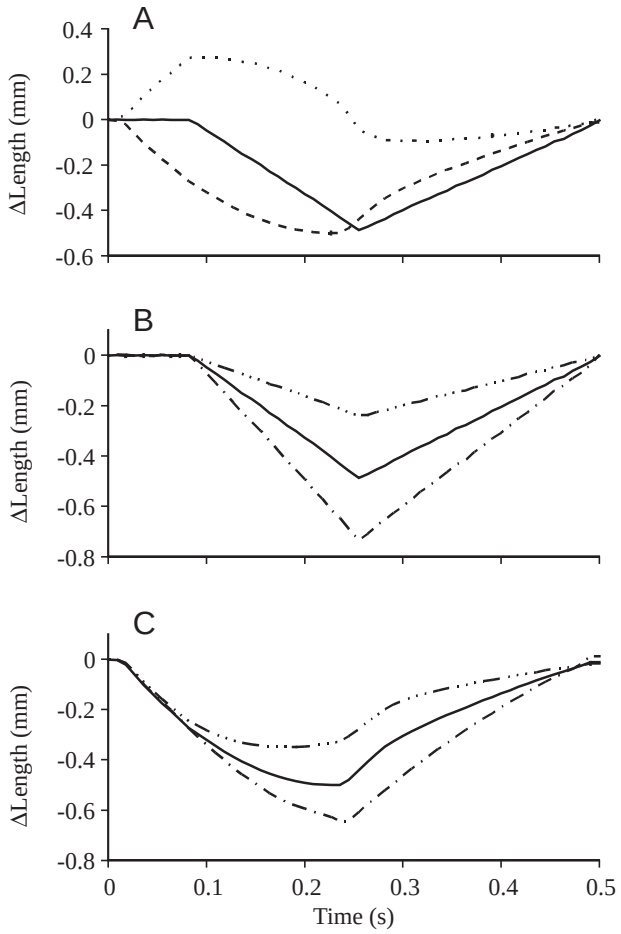

Fig. 12. Examples of the analysis of the time course of contractile component length changes. Length changes of the whole muscle (solid line) and the calculated changes in length of the contractile component (dashed line) and the series elastic component (dotted line) are shown in A. The length changes applied to the whole muscle at shortening amplitudes of 5 (top traces), 10 (middle traces) and 15 % L_{max} (bottom traces), where L_{max} is the length at which active force production is maximal, are shown in B, while C shows the calculated length changes of the contractile component only, at the same shortening amplitudes as in B. All recordings were made on the same muscle (L_{max} 4.8 mm).

It should be noted that the SEC is an integral component of papillary muscles (and all other muscles), and that the purpose of calculating contractile component length change was simply to try to understand the mechanisms underlying the constancy of energy cost.

Discussion

Isolated papillary muscles have been used extensively as a model of cardiac muscle, but in few studies has any attempt been made to use a contraction protocol that matches the strain pattern occurring in either the muscle of the ventricular wall or the papillary muscles themselves. Using the current protocol, it was possible to alter the amplitude of shortening (which would occur with stroke volume changes), the duration of the isometric phase at the start of systole (simulating changes in peak systolic pressure) and the fraction of the cycle occupied by shortening. The latter characteristic enabled contraction frequency to be increased without diminishing power output. The results of the present study indicate clearly that the variable that influenced work output per twitch to the greatest extent was the amplitude of shortening (Fig. 5). This variable can be controlled using the realistic protocol, whereas in afterloaded isotonic protocols the amount of shortening varies inversely with the afterload. No other published contraction protocol allows all the above-mentioned variables to be controlled. Furthermore, incorporating an isometric relaxation phase into the protocol produced force/length loops (Fig. 4) that closely resemble the pressure/volume loops recorded from intact beating hearts (Sagawa et al., 1988; Taylor et al., 1993). Therefore, the strain protocol demonstrated in this study has the potential to allow more sophisticated analyses of cardiac muscle function *in vitro* than has been possible with more conventional protocols.

Effects of varying contraction frequency in realistic and sinusoidal protocols

The present study tested the effects of increasing the contraction frequency from 2 Hz to 3 Hz (experiment 3). In this experiment, the power output (work output × cycle frequency) of the muscle increased by approximately 20 % and was accompanied by only a small decline in ε_{Net}. This protocol allowed us to manipulate the length changes so that the durations of the shortening and lengthening periods could be set to allow adequate time for the muscle to complete contracting before being stretched back to its resting length. In sinusoidal protocols, both power output (Baxi et al., 2000; Layland et al., 1995) and ε_{Net} (Baxi et al., 2000) decreased substantially when contraction rate was increased because of the symmetrical strain pattern of that protocol. As contraction frequency was increased, the time for both shortening and lengthening was reduced (Baxi et al., 2000; Layland et al., 1995), and relaxation was not complete prior to the muscle being stretched back to its resting length (Baxi et al., 2000). Thus, more work was required to stretch the muscle, reducing the net work performed (Baxi et al., 2000; Josephson, 1993).

In the present study, work output per twitch did decrease when contraction frequency was increased, but only slightly. The reduction in work output occurred despite there being adequate time for force output to decline to resting levels before the lengthening phase occurred. How can the decrease in work output and maintenance of enthalpy output per twitch observed to accompany an increase in contraction frequency be explained? The constancy of enthalpy output implies that the total amount of ATP used in each twitch, by both ion pumps and cross-bridges, remained constant. Although the metabolic changes that might be expected with increased contraction frequency (e.g. increased intracellular concentrations of inorganic phosphate and hydrogen ions) could have slightly reduced the molar enthalpy output of phosphocreatine hydrolysis (Woledge and Reilly, 1988), any such effect would strengthen the argument that the total amount of ATP used did not decrease significantly with the increase in contraction frequency.

In rat cardiac muscle, increasing contraction frequency is sometimes associated with a decrease in the amount of Ca^{2+} released in each twitch; e.g. Frampton et al. (Frampton et al., 1991). This could account for a lower force, and hence work, output but would also be expected to result in a proportional reduction in total energy output. The expected changes in the concentrations of metabolites do have the potential to alter force output without necessarily reducing the total number of ATP-splitting cross-bridge cycles. An increased contraction rate is associated with an increase in inorganic phosphate concentration and acidosis (Elliott et al., 1994), both of which cause a decrease in force output in cardiac muscle (Palmer and Kentish, 1996). It has been suggested that increased concentrations of inorganic phosphate and hydrogen ions alter the equilibrium between the populations of attached but non-force-generating and force-generating cross-bridges, favouring the low-force state (Hibberd et al., 1985; Kentish, 1991; Palmer and Kentish, 1996). To be consistent with the present observations, the total number of cross-bridges completing ATP splitting cycles would have had to remain unaltered, despite any differences in the equilibrium between the attached states.

Efficiency of rat papillary muscle

The maximum net mechanical efficiency of rat papillary muscle using this protocol was approximately 12 % when the muscle shortened by 10 % L_{max} and approximately 16 % when shortening was 15 % L_{max}. These values are comparable with those reported for cardiac muscle of frog and rat performing sinusoidal length change protocols (Baxi et al., 2000; Mellors et al., 2001; Syme, 1994). The values are lower than those reported for rat papillary muscles during isotonic contractions, in which efficiency was stated to be 20–25 %; e.g. Gibbs and Chapman (Gibbs and Chapman, 1979) and Kiriazis and Gibbs (Kiriazis and Gibbs, 1995). However, it has recently been demonstrated that the apparently high values can be reconciled with the lower values by correctly taking account of the pre-load when calculating work output in isotonic protocols

(Mellors et al., 2001). When this is done, the values of all the studies are consistent, with a maximum efficiency of approximately 15 %.

It was suggested previously that the difference between reported values for the maximum net mechanical efficiency of intact hearts [approximately 20–25 %, e.g. Elzinga and Westerhof (Elzinga and Westerhof, 1980) and Gibbs et al. (Gibbs et al., 1980)] and isolated papillary muscles [approximately 15 % (Baxi et al., 2000; Mellors et al., 2001)] might be reconciled if measurements with isolated muscles were made using a more realistic strain protocol (Mellors et al., 2001). However, the results of the present study are consistent with the notion that the maximum efficiency of papillary muscles is indeed approximately 15 %, regardless of protocol used. The reasons for the difference between the efficiencies of intact hearts and isolated muscles remain unclear.

Why was the energy cost per twitch unaffected by changes in strain pattern?

A striking observation from these experiments was that, at a given frequency, the enthalpy output per twitch varied little, despite the various alterations made to the protocol. As a result, changes in ε_{Net} primarily reflected changes in work output.

In experiment 1, the applied shortening velocities ranged between 0.5 and $1.0\,L_{max}\,s^{-1}$. This is a small range of shortening velocities compared with the complete range of velocities that can be attained *in vitro* using isotonic contractions. However, since the amplitude of shortening and the proportion of the cycle duration occupied by shortening were obtained from *in situ* measurements, the range of velocities used in this study corresponds to those experienced *in vivo*. As mentioned previously, the maximum shortening velocity (V_{max}) of rat papillary muscle is approximately $3.25\,L_{max}\,s^{-1}$ at 27 °C. Velocities of 0.5 and $1.0\,L_{max}\,s^{-1}$ thus correspond to approximately $0.15V_{max}$ and $0.3V_{max}$, respectively. It appears likely, therefore, that papillary muscles operate over only a small fraction of the complete range of shortening velocities, and any inherent velocity-dependence of enthalpy output would be unlikely to be apparent using this protocol. The calculated time courses of change in contractile component length indicated that the insensitivity of the enthalpy output per twitch to the pattern of applied length changes was not due to the contractile component undergoing the same pattern of length changes in all cases.

It has been proposed that the energy cost of a cardiac twitch is insensitive to the pattern of mechanical activity during the twitch because cross-bridge kinetics are sufficiently slow that there is only enough time for each cross-bridge to perform a single cycle (Gibbs and Barclay, 1998; Rossmanith et al., 1986). Countering this idea is the observation that energy cost per twitch varies considerably with afterload in isotonic contractions (Kiriazis and Gibbs, 2000). However, isotonic contractions are difficult to interpret because of the variable time spent in an isometric state at the beginning of the contraction and the variation of shortening amplitude with afterload.

When the contractile filaments slide past one another during shortening, cross-bridges would be expected to detach when they are drawn sufficiently past the position at which their free energy is minimal. If they were then to reattach to another binding site further along the actin filament and split ATP in each cycle, more ATP would be hydrolysed in each twitch and the enthalpy output would be greater. The current results, and those of earlier investigations (Gibbs and Gibson, 1970; Holroyd and Gibbs, 1992), show that this is not the case; at best, there is only a very modest increase in enthalpy output per twitch between isometric and shortening contractions (compare values in Table 1 with those in Fig. 5). Thus, if cross-bridges do perform more cycles when a papillary muscle shortens than when it contracts isometrically, the cycles must not be accompanied by ATP splitting. Ideas of this kind have been proposed to account for the decline in rate of enthalpy output with increasing velocity often observed at high shortening velocities in skeletal muscle (Barclay, 1999; Huxley, 1973). An alternative explanation is that cross-bridges in cardiac muscle are unlikely to reattach to another binding site once they have detached. This idea is the basis of most models devised to account for the cardiac muscle phenomenon of shortening deactivation. Briefly, it is envisaged that, when a cross-bridge detaches at any time in a twitch other than the first 20 % of twitch duration, the probability of reattachment is low. This is likely to be a consequence of the combination of low intracellular Ca^{2+} levels at these times and the tension dependence of Ca^{2+}–troponin binding [for a review, see Hunter et al. (Hunter et al., 1998)].

Isometric relaxation

To simulate *in vivo* ventricular muscle length changes, the linear length change protocol was modified to include an isometric relaxation phase. This modification resulted in force/length (work) loops that resemble the pressure/volume loops of the intact ventricle (Sagawa et al., 1988). Initially, it was hypothesised that the force might increase when controlled shortening was abruptly stopped since the muscle was still actively generating force. However, force continued to decline steadily with time despite the abrupt cessation of shortening (Fig. 10C). This observation is consistent with the shortening-induced deactivation described above for cardiac muscle. Incorporating the isometric relaxation phase did not greatly affect the energetics of contraction. The ability to include an isometric relaxation phase allows the protocol developed in this study to simulate changes in end-systolic volume, which is not easily achieved using conventional protocols.

Comparison with studies of energy use in whole hearts

Using an excised, whole-heart model, Suga and colleagues have consistently reported a linear relationship between the pressure/volume area (PVA) and the rate of oxygen consumption (i.e. energy cost) in the left ventricle of dogs [reviewed by Suga (Suga, 1990)]. It should be noted that the PVA includes not only the work loop, as calculated in the present study, but also a ‘potential energy’ term that is enclosed

by the extrapolation of both the active and passive pressure/volume relationships to zero pressure. For papillary muscles, the two-dimensional analogue of PVA is the force/length area (FLA). There is also a linear relationship between FLA and the rate of oxygen consumption (Hisano and Cooper, 1987; Mast and Elzinga, 1990). Thus, both PVA and FLA provide indices of the energy cost of a cardiac twitch (Taylor et al., 1993).

The alteration in strain pattern that was likely to have had the greatest effect on FLA in the present study was altering the amplitude of shortening (see Fig. 4A). An estimate was made of the difference in FLA for contractions with the greatest and smallest amplitude length changes shown in Fig. 4A. Data about the form of the FLA for rat papillary muscles were taken from Kiriazis and Gibbs (Kiriazis and Gibbs, 2000). It was estimated that FLA for a shortening amplitude of 15 % L_{max} would have been approximately 90 % of that for the 5 % L_{max} shortening. If it is assumed that the dimensionless slope of the relationship between enthalpy per beat and FLA is 2.5 and that the enthalpy output when extrapolated to an FLA of zero is 4 mJ g^{-1} (Kiriazis and Gibbs, 2000), then the difference in energy cost per beat between shortening amplitudes of 5 and 15 % L_{max} would have been only approximately 1 %. Such a small difference would be undetectable using our, or any other, method. Thus, the observed constancy of energy cost per beat in the face of substantial changes in shortening amplitude does not conflict with the idea that FLA, or PVA, provides a good index of energy cost for cardiac muscle.

This work was supported by the National Health and Medical Research Council of Australia.

References

Armour, J. A. and Randall, W. C. (1970). Electrical and mechanical activity of papillary muscle. *Am. J. Physiol.* **218**, 1710–1717.

Barclay, C. J. (1994). Efficiency of fast- and slow-twitch muscles of the mouse performing cyclic contractions. *J. Exp. Biol.* **193**, 65–78.

Barclay, C. J. (1999). A weakly coupled version of the Huxley crossbridge model can simulate energetics of amphibian and mammalian skeletal muscle. *J. Muscle Res. Cell Motil.* **20**, 163–176.

Barclay, C. J., Arnold, P. D. and Gibbs, C. L. (1995). Fatigue and heat production in repeated contractions of mouse skeletal muscle. *J. Physiol., Lond.* **488**, 741–752.

Baxi, J., Barclay, C. J. and Gibbs, C. L. (2000). Energetics of rat papillary muscle during contractions with sinusoidal length changes. *Am. J. Physiol.* **278**, H1545–H1554.

Brady, A. J. (1971). A measurement of the active state in heart muscle. *Cardiovasc. Res.* **1 (Suppl. 1)**, 11–17.

Cronin, R., Armour, J. A. and Randall, W. C. (1969). Function of the in-situ papillary muscle in the canine left ventricle. *Circ. Res.* **25**, 67–75.

Curtin, N. A. and Woledge, R. C. (1993). Efficiency of energy conversion during sinusoidal movement of white muscle fibres from the dogfish *Scyliorhinus canicula*. *J. Exp. Biol.* **183**, 137–147.

Donald, T. C., Reeves, D. N., Reeves, R. C., Walker, A. A. and Hefner, L. L. (1980). Effect of damaged ends in papillary muscle preparations. *Am. J. Physiol.* **238**, H14–H23.

Drexler, H., Flaim, S. F., Fields, R. H. and Zelis, R. (1985). Effects of nisoldipine on cardiocirculatory dynamics and cardiac output in conscious rats at rest and during treadmill exercise. *J. Pharmac. Exp. Ther.* **232**, 376–381.

Elliott, A. C., Smith, G. L. and Allen, D. G. (1994). The metabolic consequences of an increase in the frequency of stimulation in isolated ferret hearts. *J. Physiol., Lond.* **474**, 147–159.

Elzinga, G. and Westerhof, N. (1980). Pump function of the feline left heart: changes with heart rate and its bearing on the energy balance. *Cardiovasc. Res.* **14**, 81–92.

Frampton, J. E., Harrison, S. M., Boyett, M. R. and Orchard, C. H. (1991). Ca^{2+} and Na^{+} in rat myocytes showing different force–frequency relationships. *Am. J. Physiol.* **261**, C739–C750.

Gibbs, C. L. and Barclay, C. J. (1998). Efficiency of skeletal and cardiac muscle. *Adv. Exp. Med. Biol.* **453**, 527–535.

Gibbs, C. L. and Chapman, J. B. (1979). Cardiac energetics. In *Handbook of Physiology – The Cardiovascular System I*, vol. 1 (ed. R. M. Berne, N. Sperelakis and S. Geiger), pp. 775–804. Bethesda, MA: American Physiological Society.

Gibbs, C. L. and Gibson, W. R. (1970). Energy production in cardiac isotonic contractions. *J. Gen. Physiol.* **56**, 732–750.

Gibbs, C. L., Mommaerts, W. F. and Ricchiuti, N. V. (1967). Energetics of cardiac contractions. *J. Physiol., Lond.* **191**, 25–46.

Gibbs, C. L., Papadoyannis, D. E., Drake, A. J. and Noble, M. I. (1980). Oxygen consumption of the nonworking and potassium chloride-arrested dog heart. *Circ. Res.* **47**, 408–417.

Gorman III, J. H., Gupta, K. B., Streicher, J. T., Gorman, R. C., Jackson, B. M., Ratcliffe, M. B., Bogen, D. K. and Edmunds, L. H., Jr (1996). Dynamic three-dimensional imaging of the mitral valve and left ventricle by rapid sonomicrometry array localization. *J. Thorac. Cardiovasc. Surg.* **112**, 712–726.

Henderson, A. H., Craig, R. J., Sonnenblick, E. H. and Urschel, C. W. (1970). Species differences in intrinsic myocardial contractility. *Proc. Soc. Exp. Biol. Med.* **134**, 930–932.

Hibberd, M. G., Dantzig, J. A., Trentham, D. R. and Goldman, Y. E. (1985). Phosphate release and force generation in skeletal muscle fibers. *Science* **228**, 1317–1319.

Hill, A. V. (1931). Myothermic experiment on a frog gastrocnemius. *Proc. R. Soc. Lond.* **109**, 267–303.

Hirakawa, S., Sasayama, S., Tomoike, H., Crozatier, B., Franklin, D., McKown, D. and Ross, J., Jr (1977). *In situ* measurement of papillary muscle dynamics in the dog left ventricle. *Am. J. Physiol.* **233**, H384–H391.

Hisano, R. and Cooper, G. (1987). Correlation of force–length area with oxygen consumption in ferret papillary muscle. *Circ. Res.* **61**, 318–328.

Holroyd, S. M. and Gibbs, C. L. (1992). Is there a shortening-heat component in mammalian cardiac muscle contraction? *Am. J. Physiol.* **262**, H200–H208.

Hunter, P. J., McCulloch, A. D. and ter Keurs, H. E. (1998). Modelling the mechanical properties of cardiac muscle. *Prog. Biophys. Mol. Biol.* **69**, 289–331.

Huxley, A. F. (1973). A note suggesting that the cross-bridge attachment during muscle contraction may take place in two stages. *Proc. R. Soc. Lond. B* **183**, 83–86.

Josephson, R. K. (1993). Contraction dynamics and power output of skeletal muscle. *Annu. Rev. Physiol.* **55**, 527–546.

Karas, S. and Elkins, R. C. (1970). Mechanism of function of the mitral valve leaflets, chordae tendineae and left ventricular papillary muscles in dogs. *Circ. Res.* **26**, 689–696.

Kentish, J. C. (1991). Combined inhibitory actions of acidosis and phosphate on maximum force production in rat skinned cardiac muscle. *Pflügers Arch.* **419**, 310–318.

Kiriazis, H. and Gibbs, C. L. (1995). Papillary muscles split in the presence of 2,3-butanedione monoxime have normal energetic and mechanical properties. *Am. J. Physiol.* **269**, H1685–H1694.

Kiriazis, H. and Gibbs, C. L. (2000). Effects of aging on the work output and efficiency of rat papillary muscle. *Cardiovasc. Res.* **48**, 111–119.

Kretzschmar, K. M. and Wilkie, D. R. (1972). A new method for absolute heat measurement, utilizing the Peltier effect. *J. Physiol., Lond.* **224**, 18P–21P.

Layland, J., Young, I. S. and Altringham, J. D. (1995). The effect of cycle frequency on the power output of rat papillary muscles *in vitro*. *J. Exp. Biol.* **198**, 1035–1043.

Marzilli, M., Sabbah, H. N., Goldstein, S. and Stein, P. D. (1985). Assessment of papillary muscle function in the intact heart. *Circulation* **71**, 1017–1022.

Marzilli, M., Sabbah, H. N., Lee, T. and Stein, P. D. (1980). Role of the papillary muscle in opening and closure of the mitral valve. *Am. J. Physiol.* **238**, H348–H354.

Mast, F. and Elzinga, G. (1990). Heat released during relaxation equals force–length area in isometric contractions of rabbit papillary muscle. *Circ. Res.* **67**, 893–901.

Mellors, L. J., Gibbs, C. L. and Barclay, C. J. (2001). Comparison of the efficiency of rat papillary muscles during afterloaded isotonic contractions and contractions with sinusoidal length changes. *J. Exp. Biol.* **204**, 1765–1174.

Miyazaki, S., Guth, B. D., Miura, T., Indolfi, C., Schulz, R. and Ross, J., Jr (1990). Changes of left ventricular diastolic function in exercising dogs without and with ischemia. *Circulation* **81**, 1058–1070.

Mullin, W. J., Herrick, R. E., Valdez, V. and Baldwin, K. M. (1984). Adaptive responses of rats trained with reductions in exercise heart rate. *J. Appl. Physiol.* **56**, 1378–1382.

Palmer, S. and Kentish, J. C. (1996). Developmental differences and regional similarities in the responses of rat cardiac skinned muscles to acidosis, inorganic phosphate and caffeine. *J. Mol. Cell. Cardiol.* **28**, 797–805.

Paul, R. J. (1983). Physical and biochemical energy balance during an isometric tetanus and steady state recovery in frog sartorius at 0 °C. *J. Gen. Physiol.* **81**, 337–354.

Peterson, J. N., Hunter, W. C. and Berman, M. R. (1989). Control of segment length or force in isolated papillary muscle: an adaptive approach. *Am. J. Physiol.* **256**, H1726–H1734.

Ravens, U. (1992). Post-rest potentiation and its decay. In *The Interval–Force Relationship of the Heart: Bowditch Revisited* (ed. M. I. M. Noble and W. A. Seed), pp. 245–258. Cambridge: Cambridge University Press.

Rayhill, S. C., Daughters, G. T., Castro, L. J., Niczyporuk, M. A., Moon, M. R., Ingels, N. B., Jr, Stadius, M. L., Derby, G. C., Bolger, A. F. and Miller, D. C. (1994). Dynamics of normal and ischemic canine papillary muscles. *Circ. Res.* **74**, 1179–1187.

Rossmanith, G. H., Hoh, J. F., Kirman, A. and Kwan, L. J. (1986). Influence of V1 and V3 isomyosins on the mechanical behaviour of rat papillary muscle as studied by pseudo-random binary noise modulated length perturbations. *J. Muscle Res. Cell Motil.* **7**, 307–319.

Sagawa, K., Maughan, L., Suga, H. and Sunagawa, K. (1988). *Cardiac Contraction and the Pressure–Volume Relationship*. New York: Oxford University Press, Inc.

Semafuko, W. E. B. and Bowie, W. C. (1975). Papillary muscle dynamics: *in situ* function and responses of the papillary muscle. *Am. J. Physiol.* **228**, 1800–1807.

Sonnenblick, E. H. (1964). Series elastic and contractile elements in heart muscle: changes in muscle length. *Am. J. Physiol.* **207**, 1330–1338.

Suga, H. (1990). Ventricular energetics. *Physiol. Rev*. **70**, 247–277.

Syme, D. A. (1994). The efficiency of frog ventricular muscle. *J. Exp. Biol.* **197**, 143–164.

Taylor, T. W., Goto, Y. and Suga, H. (1993). Variable cross-bridge cycling-ATP coupling accounts for cardiac mechanoenergetics. *Am. J. Physiol*. **264**, H994–H1004.

Woledge, R. C., Curtin, N. A. and Homsher, E. (1985). *Energetic Aspects of Muscle Contraction.* 357p. London: Academic Press.

Woledge, R. C. and Reilly, P. J. (1988). Molar enthalpy change for hydrolysis of phosphorylcreatine under conditions in muscle cells. *Biophys. J*. **54**, 97–104.